OPEN ACCESS
Journal of Innovative Optical Health Sciences
Vol. 17, No. 2 (2024) 2350023 (12 pages)

DOI: 10.1142/S1793545823500232

World Scientific
www.worldscientific.com

Tissue optical clearing enhances efficacy of vascular targeted photodynamic therapy of mouse dorsal skin

Ying Liu*, Qiushi Wang†, Yidi Liu‡, Ying Wang‡, Haixia Qiu‡, Dan Zhu§, Ying Gu†,‡,¶ and Defu Chen†,‖

*School of Optics and Photonics, Beijing Institute of Technology, Beijing 100081, P. R. China

†School of Medical Technology, Beijing Institute of Technology, Beijing 100081, P. R. China

‡Department of Laser Medicine, First Medical Center of PLA General Hospital, Beijing 100853, P. R. China

§Britton Chance Center for Biomedical Photonics – MoE Key Laboratory for Biomedical Photonics, Advanced Biomedical Imaging Facility, Wuhan National Laboratory for Optoelectronics, Huazhong University of Science and Technology, Wuhan 430074, Hubei, P. R. China

¶Precision Laser Medical Diagnosis and Treatment Innovation Unit, Chinese Academy of Medical Sciences, Beijing 100000, P. R. China

‖defu@bit.edu.cn

Received 20 April 2023
Revised 26 July 2023
Accepted 26 July 2023
Published 30 August 2023

Vascular-targeted photodynamic therapy (V-PDT) is an effective treatment for port wine stains (PWS). However, repeated treatment is usually needed to achieve optimal treatment outcomes, possibly due to the limited treatment light penetration depth in the PWS lesion. The optical clearing technique can increase light penetration in depth by reducing light scattering. This study aimed to investigate the V-PDT in combination with an optical clearing agent (OCA) for the therapeutic enhancement of V-PDT in the rodent skinfold window chamber model. Vascular responses were closely monitored with laser speckle contrast imaging (LSCI), optical coherence tomography angiography, and stereo microscope before, during, and after the treatment. We further quantitatively demonstrated the effects of V-PDT in combination with OCA on the blood flow and blood vessel size of skin microvasculature. The combination of OCA and V-PDT resulted in significant vascular damage, including vasoconstriction and the reduction of blood flow.

‖Corresponding author.

Our results indicate the promising potential of OCA for enhancing V-PDT for treating vascular-related diseases, including PWS.

Keywords: Vascular-targeted photodynamic therapy (V-PDT); optical clearing agent (OCA); treatment efficacy; enhancement; skin-fold window chamber; port wine stains.

1. Introduction

Port wine stains (PWS) are congenital and progressive capillary malformations and affect 0.3–0.5% of the population.[1] PWS lesions are most commonly located on the head and face regions and can progressively deepen in color with age and develop tissue hypertrophy and nodularity if left untreated.[2,3] Vascular-targeted photodynamic therapy (V-PDT) has proven to be a safe and effective treatment for PWS and has been successfully used to treat PWS in China since 1991.[4–8] The therapy involves the intravenous administration of a photosensitizer followed by light illumination of the PWS lesion area with laser light at an appropriate wavelength to activate the photosensitizer. Activating the photosensitizer in the presence of oxygen triggers a series of photochemical reactions and produces intravascular cytotoxic singlet oxygen, which damages vascular endothelial cells and eventually leads to target vascular closure without destroying surrounding normal tissues.[9–11] V-PDT has also been used to prevent or treat other vascular-related diseases, including age-related macular degeneration (AMD) and pancreatic and prostate cancers.[12–15]

Although V-PDT is an effective treatment modality for PWS, repeated V-PDT treatment is usually needed in most PWS patients to obtain an optimal treatment outcome, especially for the purplish-red or thickened types.[9,10,16] This may be due to the limited treatment light penetration depth in the PWS lesion. The 532 nm laser light combined with the photosensitizer hematoporphyrin monomethyl ether (HMME) is often used to treat PWS.[17–19] The 532 nm green laser light is highly scattered through the skin and absorbed primarily by more superficial cutaneous vessels. Hence, an insignificant quantity of green laser light reaches the deeper dilated malformed vascular.[20]

One approach to improve the V-PDT treatment for PWS would be to change the optical characteristics of the skin, improving the light penetration. Optical clearing techniques can make the *in vivo* skin optically transparent.[21,22] Optical clearing agent (OCA) can increase the light penetration depth without increasing power, avoiding producing unacceptable tissue heating. Because of the matching of refractive indices between tissue components and interstitial fluid changed by an OCA diffused into the tissue, the optical clearing technique can decrease light scattering and improve the light penetration depth.[23] A previous study showed that a mixture of PEG-400, sucrose, and thiazone has the optimal capacity to enhance imaging performance.[24] Our previous study also showed that topical application of this OCA improves the imaging depth and contrast of optical coherence tomography angiography in PWS patients and increases the imaging depth in human opisthenar skin by approximately 0.16 ± 0.03 mm.[25] The skins recovered quickly after applying normal saline both *in vivo* in mouse and human skin.[24,25] With repetitive use of this OCA, no side effects were observed on the skin. Previous studies have also demonstrated that the combination of OCA and PDT can improve the effectiveness of PDT in treating melanoma in an immunocompromised mouse model *in vivo*.[26,27] Due to a resultant refractive index matching, OCA-treated tumors are more optically homogenous, improving the PDT response.[28] Their results showed that topical application of OCA reduces the light scattering at the cutaneous melanoma model, increasing the light penetration in depth. However, it remains unknown whether V-PDT, in combination with OCA, may improve the effects of V-PDT in the skin.

In this study, we aimed to investigate the V-PDT in combination with OCA for enhancing V-PDT-induced vascular damage in the rodent skinfold window chamber model. Vascular responses were closely monitored with laser speckle contrast imaging (LSCI), optical coherence tomography angiography (OCTA), and stereo microscope before, during, and after the V-PDT treatment. Vascular metrics, such as blood flow and blood vessel size, were quantitatively compared between the groups with

and without topical application of OCA, demonstrating the potential of OCA for enhancing V-PDT for treating vascular-related diseases, including PWS.

2. Materials and Methods

2.1. *Animal model*

Dorsal window chambers (APJ Trading Co., Ventura, CA, USA) were surgically implanted in Balb/C female mice at 21–25 g body weight (8–11 weeks, SPF (Beijing) Biotechnology Co., Ltd., China) using established methods.[29] Before surgery, the dorsal hair was carefully shaved, and the residual hair was removed by depilatory cream. In essence, the skin on one side of the window was excised, making it possible to visualize the subdermal microvasculature of the opposing skin. During surgery, mice were anesthetized with the isoflurane–oxygen mixture (1–2% at a rate of 1.0 L/min). All the animal procedures were approved by the Beijing Institute of Technology Ethical Committee.

2.2. *Skin optical clearing agents*

A new OCA designed for skin optical clearing was used in this study, and the detail for preparing this OCA has been described elsewhere.[24,25] In brief, three main agents: PEG-400, sucrose, and thiazone, were used in this study. PEG-400 was first mixed with thiazone at a volume ratio of 9:1 and then mixed with sucrose at a volume ratio of ∼1:1. It should be noted that sucrose was prepared as a saturated aqueous solution with a 67.1% mass fraction. Combining these chemical agents in this ratio has demonstrated higher *in vivo* skin optical clearing efficacy than other combinations and ratios of agents.[24]

2.3. *Study protocols*

A domestically produced photosensitizer (PS) HMME (Hemoporfin) was used in this study. Animals were randomly divided into four groups ($n = 3$ per group), i.e., V-PDT group, V-PDT+OCA group, PS+OCA group, and laser+OCA group. For the V-PDT, V-PDT+OCA, and PS+OCA groups, the animals received an intravenous administration of a 150 μl saline solution of HMME with a dose of 30 mg/kg body weight. Light irradiation was performed immediately after the intravenous injection of the photosensitizer. The microvascular treatment responses were assessed by stereo-microscope, LSCI, and OCTA. Figure 1(a) shows the schematic of the LSCI for real-time monitoring of the window chamber during laser irradiation. A 532 nm green solid-state laser (MGL-F-532 nm, Changchun New

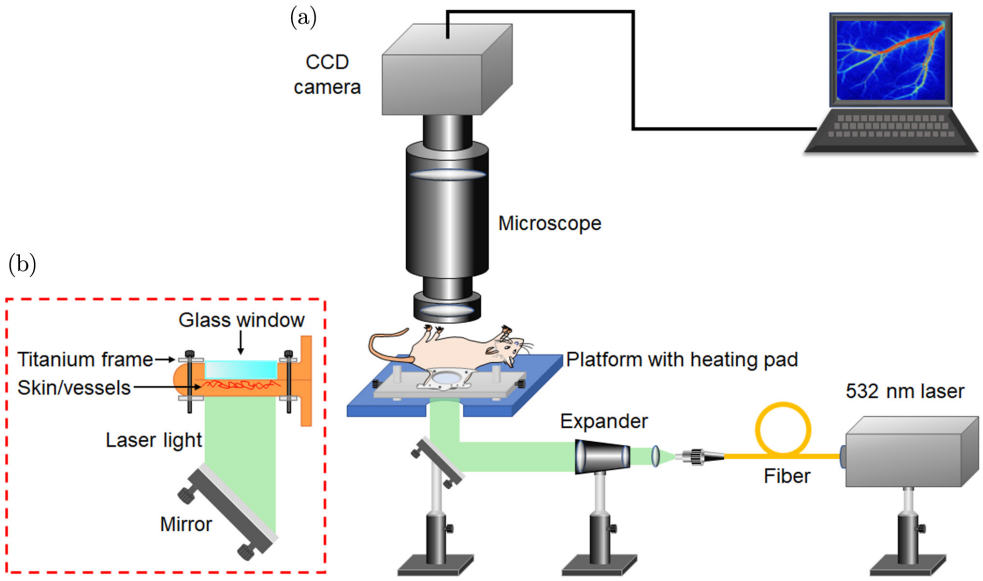

Fig. 1. Experimental setup for window chamber imaging during V-PDT. (a) Schematic of the LSCI for real-time monitoring of the window chamber during laser irradiation. (b) The 532 nm laser light was reflected by a mirror passed right through the epidermal side. The mouse was placed on a temperature-controlled heating pad (37°C) and the window chamber screws were positioned in the predrilled holes in the imaging platform plate.

Industries Optoelectronics Technology Co., Ltd., Changchun, China) was used to activate the photosensitizer with a power density of 100 mW/cm^2 and an irradiation time of 20 min, following the clinical light dose.[9–11] The 532 nm laser light passed right through the epidermal side, penetrating the skin and eventually reaching the subdermal microvascular (as shown in Fig. 1(b)). The subdermal side was positioned under the LSCI system, and the subdermal vascular changes can be readily visualized through the window. Following previous studies, OCA was applied topically on the epidermal side in the window 5 min before the intervention, and adhesive tape stripping was used to remove the *stratum corneum* before OCA application.[30,31]

During the intervention, the vascular change was closely monitored with LSCI. Before and after the intervention, the skinfold window chamber was evaluated with LSCI, OCTA, and stereo-microscope, respectively. For all the imaging procedures, the mouse was placed on a temperature-controlled heating pad (37°C) and fitted to a rodent mask to maintain anesthesia with ~1–2% isoflurane–oxygen mixture. The window chamber screws were positioned in the predrilled holes in the imaging platform plate to prevent movement during imaging.

2.4. *Laser speckle contrast imaging (LSCI)*

The LSCI system was provided by Wuhan XunWei Optoelectronic Technology Co. Ltd. The LSCI system was based on a stereo microscope body (SZ-61, Olympus, Japan). The system consisted of a continuous-wave laser source with a wavelength of 785 nm and a charge-couple device (CCD) camera (Baumer TXG03, Germany; pixel size = 7.4 × 7.4 μm^2). The CCD exposure time in this study was 31 ms. The raw data were processed to generate blood flow images based on the laser speckle temporal contrast analysis.[32]

2.5. *Optical coherence tomography angiography (OCTA)*

The swept source OCT (SS-OCT) was provided by TianJin HoriMed Medical Technology Co., Ltd. TianJin, China. An X–Y galvo-scanning mirrors were adopted in the sample arm to facilitate 3D imaging at an A-scan rate of 200 kHz. Using a swept laser source with a central wavelength of 1300 nm, an axial resolution of ~12 μm and a lateral resolution of ~9 μm can be achieved. A visible red light was coupled to the interferometer to guide SS-OCT imaging. The OCTA image of the vasculature was obtained by employing the well-established complex-based OCT angiography algorithm, which has been previously reported to deliver superior vascular imaging performance in a phase-stable system.[33]

2.6. *Data analysis*

OCTA data and white light images were analyzed using Matlab (The MathWorks, Inc.) and ImageJ (Fiji). The LSCI data were analyzed with the RTLBI software (Real-time Laser Blood Flow Imaging, Wuhan National Laboratory for Optoelectronics, Wuhan, China). Microvascular parameters, such as blood flow and blood vessel size, were quantified for each group. The blood flow of each selected blood vessel was measured three times within the region of interest in the LSCI image. Three representative veins and arteries were selected and measured to calculate the average blood flow for each mouse. The diameter of each selected blood vessel was measured three times in the white light image, and three representative veins and arteries were selected and measured to calculate the average diameter. Empirical knowledge based on the anatomic structure, blood flow velocity, and the reflection color of blood vessels was used to identify arteries and veins. Vasoconstriction of blood vessels after V-PDT was also quantified by the decrease in vascular diameter after V-PDT divided by the vascular diameter before V-PDT. Data are presented as means + standard deviations (SD). All the measured data were graphed using OriginPro 9.1 software (OriginLab Corporation, MA, USA). The paired Student's t-test was used to compare the differences immediately before, during, and after V-PDT. P-values below 0.05 were considered statistically significant.

3. Results

3.1. *In vivo assessment of vascular effects of V-PDT in combination with OCA*

Figure 2 shows the representative images for the window chamber model before and after topical

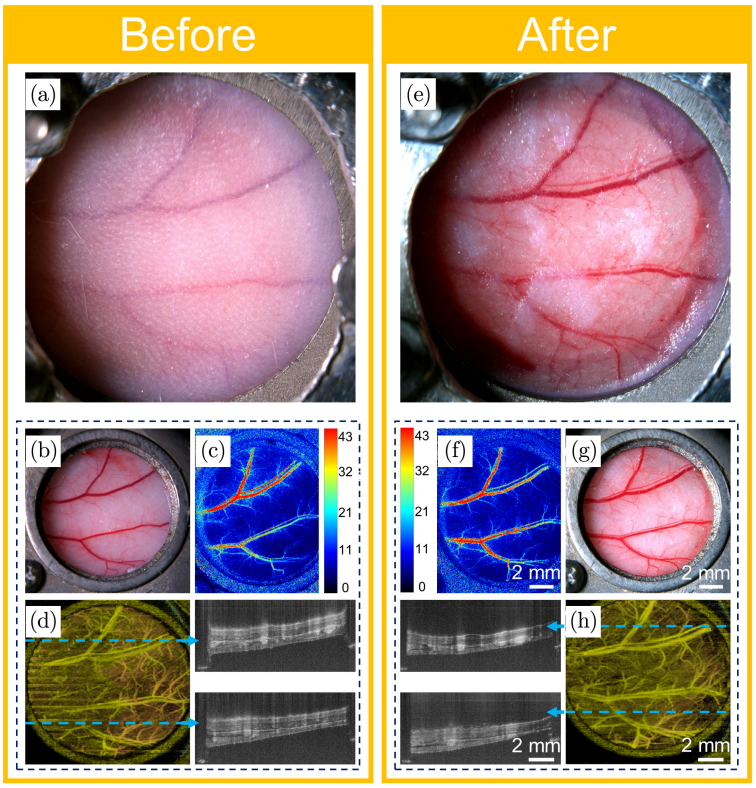

Fig. 2. Example of skinfold window chamber before and after topical application of OCA. Before: (a) White light image of the epidermal size of the skin, (b)–(d) white light image, LSCI image, and *en face* OCTA image and the cross-sectional OCTA images corresponding to the location indicated by the light blue dashed line of the subdermal size of the skin. After: (e) White light image of the epidermal size of the skin, (f)–(h) white light image, LSCI image, and *en face* OCTA image and the cross-sectional OCTA images corresponding to the location indicated by the light blue dashed line of the subdermal size of the skin.

application of OCA. Five minutes after topical application of OCA, the turbid skin on the epidermal side became transparent (Fig. 2(e)). White light images, LSCI images, and OCTA images from the subdermal side were also taken by stereo-microscope, LSCI, and OCTA, before and after the topical application of OCA. There are no apparent vasculature changes in the white light images, LSCI images, and *en face* OCTA images from the subdermal side.

Figure 3(a) shows the representative changes in blood flow with time by comparing the LSCI images immediately before, during, and after HMME-mediated V-PDT after the topical application of OCA on the window chamber. This change can also be observed from the *en face* OCTA images and the representative cross-sectional OCTA images acquired before and after V-PDT (Fig. 3(b)) and the white light images (Fig. 3(c)). As both the LSCI signal and OCTA signal are sensitive to the blood flow, the disappearance of blood vessels in the LSCI images and *en face* OCTA images may indicate the creation of blood clots or the closure of blood vessels. The blood flow and vascular diameters were further quantified (Figs. 3(d) and 3(e)). We found that the blood flow decreased remarkably 5 min after initiation of V-PDT and then remained almost disappeared throughout the treatment. The results showed that the combination of OCA and V-PDT resulted in significant vascular damage, including vasoconstriction and the reduction of blood flow. However, the blood vessels were found to have a slight recovery in blood flow and blood vessel size one hour after V-PDT.

3.2. *Comparison study of vascular effects of V-PDT with and without OCA*

Figures 4(a)–4(d) provide representative LSCI images taken from V-PDT+OCA, V-PDT, PS+OCA, and laser+OCA groups, respectively. The LSCI images were recorded immediately before (0 min), during (5 min, 10 min, 15 min, and 20 min), and after (80 min) the intervention for each group.

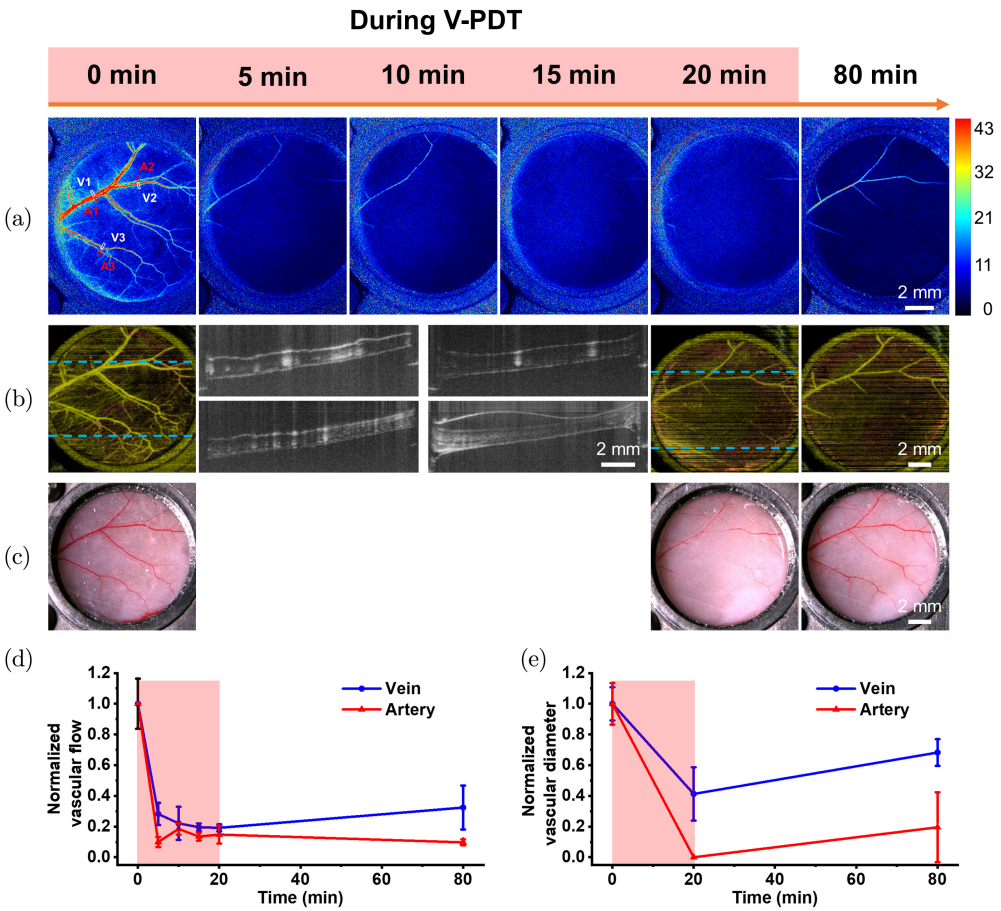

Fig. 3. Responses of the microvasculature to V-PDT (100 mW/cm^2, 20 min) after topical application of OCA. (a) LSCI vascular images immediately before V-PDT (0 min), during V-PDT (5 min, 10 min, 15 min, and 20 min), and after V-PDT (80 min). (b) OCTA images immediately before, immediately after, and one hour after V-PDT, and the cross-sectional OCTA images corresponding to the location indicated by the light blue dashed line. (c) White light images immediately before, immediately after, and one hour after V-PDT. Changes in the blood flow (d) and vascular diameters (e) for the representative blood vessels (as marked in (a)) with time. The blood flow and vascular diameters were normalized to the corresponding baseline values measured immediately before V-PDT. A: Artery, V: Vein.

The blood flow of different blood vessels was further quantified (Figs. 4(e) and 4(f)). Only the V-PDT +OCA group showed significant photodynamic effects, leading to an apparent disappearance of blood vessels and an immediate decrease in blood flow within the field of view (Fig. 4(a)). In the V-PDT alone group, a slight reduction in blood flow was observed during the 20 min V-PDT treatment, followed by a return to the pre-treatment level at one hour after V-PDT (Fig. 4(b)). In the PS+OCA group, blood flow did not change significantly across time (Fig. 4(c)). In the laser+OCA group, there was a slight increase in blood flow during laser irradiation (Fig. 4(d)). The results show that combining OCA and V-PDT can significantly enhance V-PDT-induced vascular damage, significantly reducing blood flow.

Figures 5(a)–5(d) further show the vasculature alterations by comparing the white light images and the *en face* OCTA images immediately before (0 min), immediately after (20 min), and one hour after (80 min) the intervention for each group. Vascular diameters of the artery and vein in the white light images were further quantified (Figs. 5(e) and 5(f)). Only the V-PDT+OCA group showed significant photodynamic effects, leading to a marked disappearance of vasculature within the field of view (Fig. 5(a)). For the V-PDT, PS+OCA, and laser+OCA groups, no noticeable microvascular changes were observed in the OCTA images and white light images (Figs. 5(b), 5(c) and 5(d)). This is consistent with the above LSCI results that OCA can enhance V-PDT-induced vascular damage.

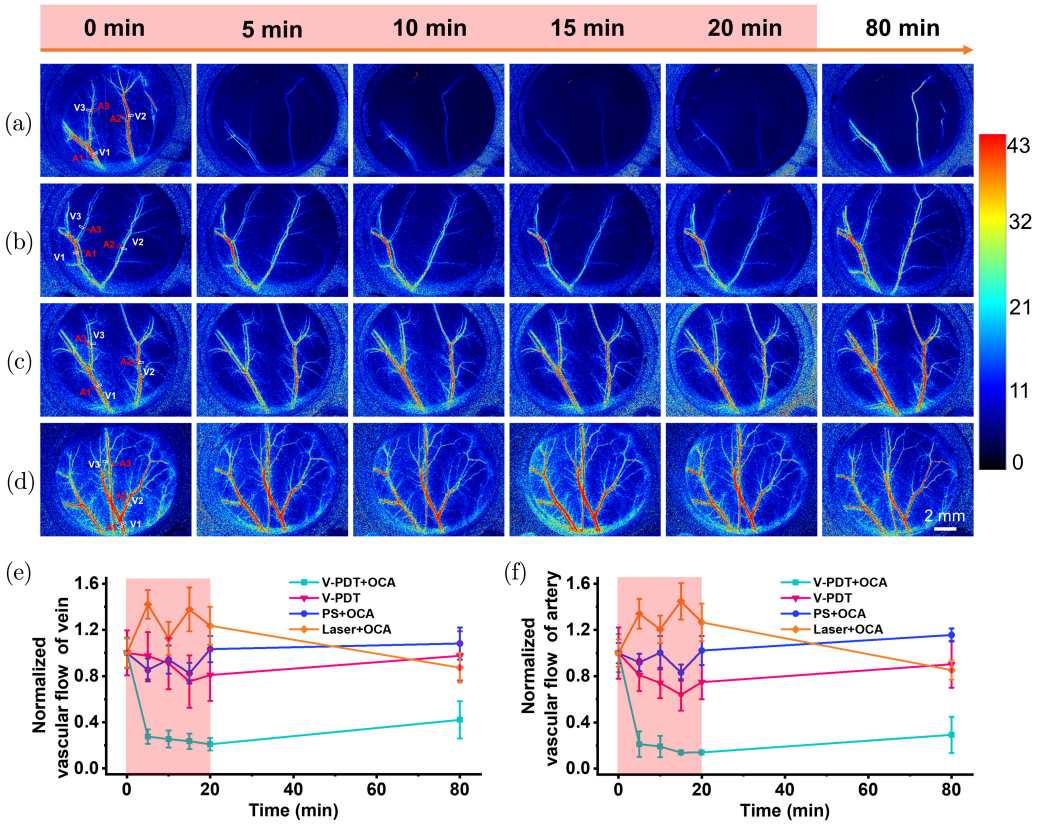

Fig. 4. Representative LSCI images of the microvasculature following interventions: (a) V-PDT+OCA, (b) V-PDT, (c) PS+OCA, and (d) Laser+OCA. Changes in the blood flow of the representative vein (e) and artery (f) (as marked in the LSCI at 0 min) with time. The blood flow was normalized to the corresponding baseline values measured immediately before intervention. V-PDT+OCA resulted in the most apparent decrease in vascular perfusion. A: Artery, V: Vein.

Figures 6(a) and 6(b) summarize the mean blood flow change of veins and arteries from the LSCI images for four experimental groups. In the V-PDT +OCA group, we found that the overall level of blood flow decreased remarkably to a lower level 5 min after initiation of V-PDT, followed by a slight decrease throughout the treatment. The veins were found to have a slight recovery in blood flow one hour after V-PDT. In the V-PDT alone group, a small reduction in blood flow was observed during the 20 min V-PDT treatment, followed by a return to the pre-treatment level at one hour after V-PDT. In the PS+OCA group, blood flow did not change significantly across time. In the laser+OCA group, there was a slight increase in flow during laser irradiation, which may be due to the local thermal effect.[10] Figures 6(c) and 6(d) further summarize the mean vascular diameter change of the artery and vein from the white light images. In the V-PDT +OCA group, the blood vessels were found to have partial vasoconstriction. For the V-PDT, PS +OCA, and laser+OCA groups, no apparent reduction in vascular diameter was found. Immediately after the intervention, the average vasoconstriction for the V-PDT+OCA group ($n = 3$) was around 24.65% for veins and 55.54% for arteries, respectively, while for the V-PDT, PS+OCA, and laser+OCA groups ($n = 3$ for each group), the average vasoconstriction was less than 7% for both veins and arteries. Taken together, these results suggest that the combination of OCA and V-PDT can significantly enhance V-PDT-induced vascular damage.

4. Discussion

PWS are congenital vascular malformations histologically characterized by ectatic capillaries, mainly in the upper dermis.[34] If left untreated, the PWS lesions tend to darken and develop nodular components and facial deformation with age.[3] V-PDT based on the local destruction of vascular is an effective treatment for PWS, and the 532 nm laser light combined with the HMME is most often used

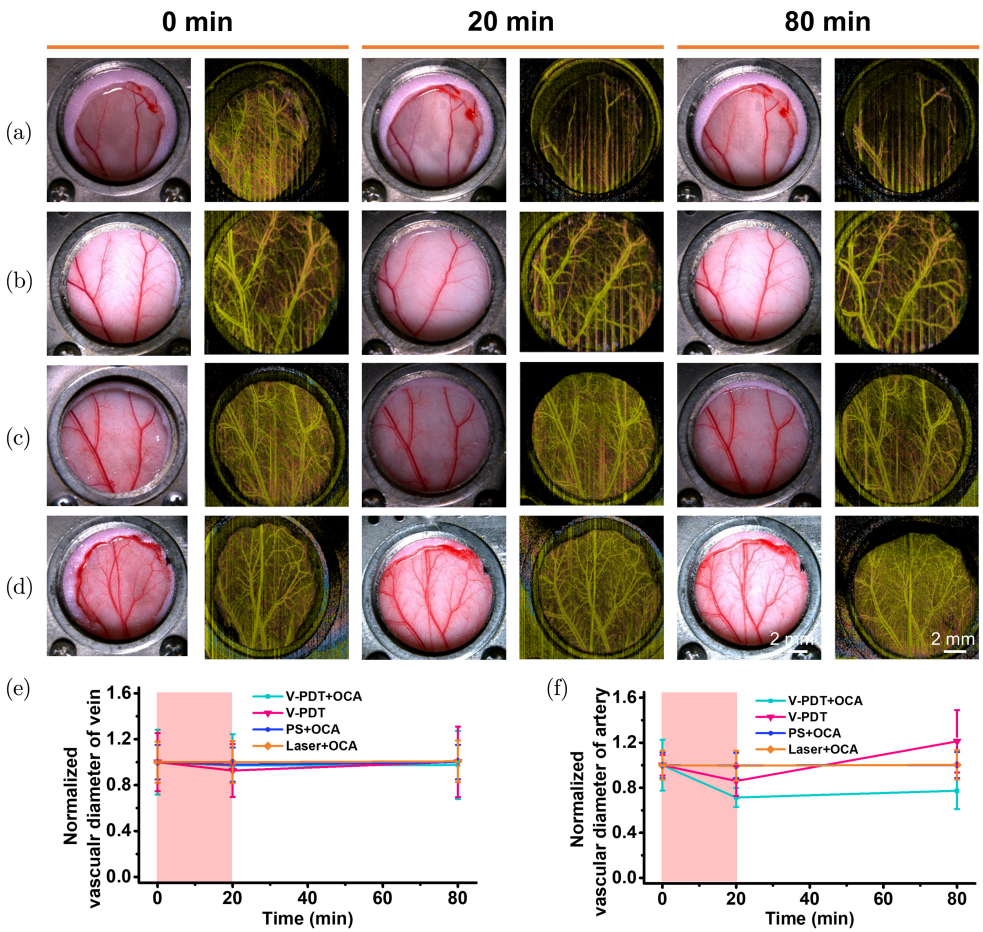

Fig. 5. Representative OCTA images and white light images of the microvasculature following interventions: (a) V-PDT+OCA, (b) V-PDT, (c) PS+OCA, and (d) Laser+OCA. Changes in the vascular diameters for the representative (e) vein and (f) artery. The vascular diameters were normalized to the corresponding baseline values measured immediately before V-PDT. Marked vascular damage is observed after treatment for the V-PDT+OCA group.

for treating PWS. However, repeated V-PDT treatment is usually needed in most PWS patients to obtain an optimal treatment outcome, possibly due to the limited treatment light penetration depth in the PWS lesion. The malformed enlarged blood vessels were predominantly located in the upper dermis of PWS, and the superficial plexuses were observed to be located at depths between 108 μm and 672 μm below the skin surface in five PWS patients by using OCT.[35] Here, we have chosen to study the effects of V-PDT in combination with OCA for vascular damage in the skinfold window chamber model. This study demonstrates the promising potential of OCA for enhancing V-PDT in the skin and provides a penitential way to improve the V-PDT treatment for PWS.

It should be noted that laser irradiation in this study was performed directly on the epidermal side of the skinfold, which is different from the subdermal irradiation previously.[36–39] Several studies have investigated the V-PDT vascular effects in the rodent skinfold window chamber model, and laser irradiations were performed directly on the subdermal side of the skinfold.[36–39] Their results have shown that V-PDT resulted in dramatic vasoconstriction and reduced blood flow by using subdermal irradiation. However, in this study, the V-PDT alone group led to slight microvascular changes through epidermal irradiation. The difference in vascular response can be attributed to different laser irradiation methods. For the epidermal irradiation, the 532 nm treatment light passed through the epidermal side, penetrating the skin and eventually reaching the subdermal microvascular. Due to light scattering and absorption of the epidermis, an insignificant amount of green laser light reaches the subdermal blood vessels. It is insufficient to generate enough intravascular singlet

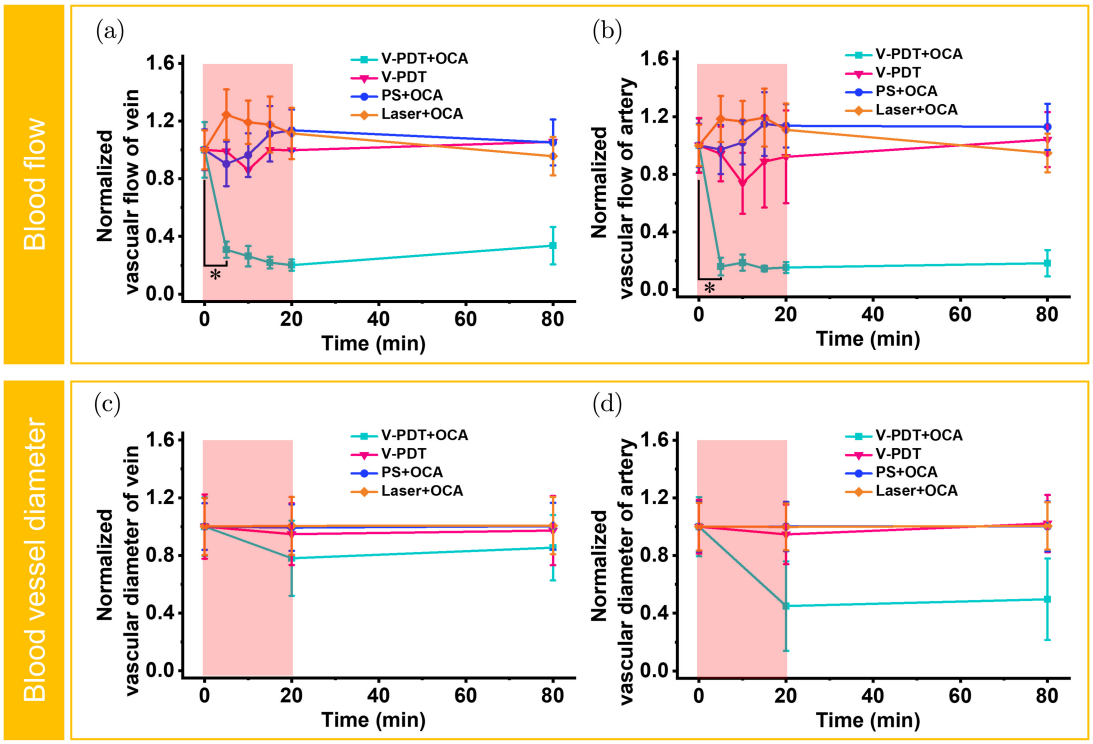

Fig. 6. Comparison study of the OCA enhanced V-PDT effects on skinfold window chamber model. Mean blood flow changes of the vein (a) and artery (b) with time for four experimental groups. Mean vascular diameters changes of vein (c) and artery (d) with time for four experimental groups. The blood flow and vascular diameters were normalized to the corresponding baseline values measured immediately before V-PDT. $n = 3$ for each group. ($^*P < 0.05$).

oxygen to cause vascular damage. Compared with the previous subdermal irradiation, the epidermal irradiation used in this study allows a better simulation of the V-PDT treatment for PWS.

The complex morphological features of the skin and the variations of the index of refraction within various internal components make the skin show a high light scatting characteristic, which attenuates the effective penetrating light intensity.[24,40] Several studies have shown that the optical clearing technique can effectively reduce the multiple scattering of light and improve the light penetration depth.[21,23,41] Our recent work has also shown that OCA has excellent efficiency in increasing light penetration depth and enhancing the quality and depth of OCTA imaging in healthy skin and PWS lesions.[25] Compared with the V-PDT alone group, the combination of OCA and V-PDT resulted in significant vascular damage, including vasoconstriction and reduced blood flow. After topical application of OCA, a more considerable amount of treatment light can reach deeper blood vessels, in which sufficient singlet oxygen is produced to damage the targeted blood vessels. Furthermore, it was observed that different types of blood vessels have different responses to V-PDT, which is in line with the previous study.[37,42] In this study, the arteries after V-PDT were found to have a higher decrease in blood flow and vascular diameter than veins. One of the possible explanations for this is the difference in vascular anatomy for different types of blood vessels.[42] The vessel wall of a vein is usually thinner than an artery of equal caliber, and the thickness of the artery and vein wall varies with the vessel caliber. Another possible explanation is the difference in the platelet aggregation initiated by the chain of photodynamic reactions.[42] The differences in the blood flow and oxygen level in arteries, and veins, may also lead to different rates in platelet aggregation and vessel occlusion.

Previous studies have shown that the combination of OCA and PDT can improve the effectiveness of PDT in treating melanoma.[26,27] Their results showed that topical application of OCA to a cutaneous melanoma model shortly before PDT can increase the effective treatment depth by reducing the light scattering.[26,27] Compared to the conventional PDT approach, V-PDT predominates through

vascular-mediate due to the short drug-light time interval used.[43] For V-PDT treatment, light treatment was performed immediately after the intravenous injection of photosensitizer, when the photosensitizer is primarily confined in the blood vessels. A new OCA designed for skin optical clearing was used in this study. Our previous studies have demonstrated that this OCA improves imaging depth and contrast of optical coherence tomography in mouse skin[24] and PWS patients.[25] In this study, this OCA was used for therapy. OCA can enhance V-PDT for selective damage to blood vessels by increasing light penetration. OCA can increase light penetration depth in PWS lesions;[25] thus, combining V-PDT and OCA has great promise in improving the V-PDT treatment for PWS. However, the safety and biocompatibility of OCAs need to be further investigated to eliminate the potential detrimental effects of OCAs before this method can be used in clinical practice.[44,45] Developing safe optical clearing methods is crucial for the clinical application of the combination of V-PDT and OCA. Recently, a few *in vivo* optical clearing studies in mouse skin or human skin can be found, showing the application perspective of OCA in the clinic.[24,25] We believe that *in vivo* optical clearing skin continues to get closer to clinical application, and the combination of V-PDT and OCA can be applied in the clinic once the OCA can be safely used *in vivo* on humans.

5. Conclusions

In summary, combining V-PDT and OCA demonstrated enhanced V-PDT effects compared to V-PDT alone in the skinfold window chamber model. Future work should investigate the relationship between light dose, photosensitizer dose, and V-PDT dose to treatment outcomes after topical application of OCA. The V-PDT+OCA approach has clinical translational potential for enhancing V-PDT for treating vascular-related diseases, particularly for PWS.

Acknowledgments

This study was supported by the National Natural Science Foundation of China (Grant Numbers 62205025 and 61835015), Beijing Natural Science Foundation (7222309), the Open Project Program of Wuhan National Laboratory for Optoelectronics (2020WNLOKF025), CAMS Innovation Fund for Medical Sciences (CIFMS) (2019-I2M-5-061), and Beijing Institute of Technology Research Fund Program for Young Scholars (XSQD-202123001).

Conflict of Interest

The authors declare that there is no conflict of interest.

References

1. J. C. Alper, L. B. Holmes, "The incidence and significance of birthmarks in a cohort of 4,641 newborns," *Pediatr. Dermatol.* **1**(1), 58–68 (1983).
2. K. M. Kelly, B. Choi, S. McFarlane, A. Motosue, B. J. Jung, M. H. Khan, J. C. Ramirez-San-Juan, J. S. Nelson, "Description and analysis of treatments for port-wine stain birthmarks," *Arch. Facial Plast. Surg.* **7**(5), 287–294 (2005).
3. S. L. Hagen, K. R. Grey, D. Z. Korta, K. M. Kelly, "Quality of life in adults with facial port-wine stains," *J. Am. Acad. Dermatol.* **76**(4), 695–702 (2017).
4. Y. Gu, N. Y. Huang, J. Liang, Y. M. Pan, F. G. Liu, "Clinical study of 1949 cases of port wine stains treated with vascular photodynamic therapy (Gu's PDT)," *Ann. Dermatol. Venereol.* **134**(3), 241–244 (2007).
5. H. Qiu, Y. Gu, Y. Wang, N. Huang, "Twenty years of clinical experience with a new modality of vascular-targeted photodynamic therapy for port wine stains," *Dermatol. Surg.* **37**(11), 1603–1610 (2011).
6. Y. Zhao, P. Tu, G. Zhou, Z. Zhou, X. Lin, H. Yang, Z. Lu, T. Gao, Y. Tu, H. Xie, Q. Zheng, Y. Gu, J. Tao, X. Zhu, "Hemoporfin photodynamic therapy for port-wine stain: a randomized controlled trial," *PLoS ONE* **11**(5), e0156219 (2016).
7. G. Ma, Y. Han, H. Ying, X. Zhang, W. Yu, J. Zhu, Q. Cen, H. Chen, Y. Jin, X. Lin, "Comparison of two generation photosensitizers of PsD-007 and hematoporphyrin monomethyl ether photodynamic therapy for treatment of port-wine stain: a retrospective study," *Photobiomodul. Photomed. Laser Surg.* **37**(6), 376–380 (2019).
8. D. Chen, Y. Wang, H. Zhao, H. Qiu, Y. Wang, J. Yang, Y. Gu, "Monitoring perfusion and oxygen saturation in port-wine stains during vascular targeted photodynamic therapy," *Ann. Transl. Med.* **9**(3), 214 (2021).
9. J. Ren, P. Li, H. Zhao, D. Chen, J. Zhen, Y. Wang, Y. Wang, Y. Gu, "Assessment of tissue perfusion changes in port wine stains after vascular targeted

photodynamic therapy: a short-term follow-up study," *Lasers Med. Sci.* **29**(2), 781–788 (2014).
10. D. Chen, J. Ren, Y. Wang, B. Li, Y. Gu, "Intraoperative monitoring of blood perfusion in port wine stains by laser Doppler imaging during vascular targeted photodynamic therapy: A preliminary study," *Photodiagnosis Photodyn. Ther.* **14**, 142–151 (2016).
11. D. Chen, W. Yuan, H.-C. Park, X. Li, "*In vivo* assessment of vascular-targeted photodynamic therapy effects on tumor microvasculature using ultrahigh-resolution functional optical coherence tomography," *Biomed. Opt. Exp.* **11**(8), 4316–4325 (2020).
12. H. T. Sjoberg, Y. Philippou, A. L. Magnussen, I. D. C. Tullis, E. Bridges, A. Chatrian, J. Lefebvre, K. H. Tam, E. A. Murphy, J. Rittscher, D. Preise, L. Agemy, T. Yechezkel, S. C. Smart, P. Kinchesh, S. Gilchrist, D. P. Allen, D. A. Scheiblin, S. J. Lockett, D. A. Wink, A. D. Lamb, I. G. Mills, A. Harris, R. J. Muschel, B. Vojnovic, A. Scherz, F. C. Hamdy, R. J. Bryant, "Tumour irradiation combined with vascular-targeted photodynamic therapy enhances antitumour effects in pre-clinical prostate cancer," *Br. J. Cancer* **125**(4), 534–546 (2021).
13. A.-R. Azzouzi, S. Vincendeau, E. Barret, A. Cicco, F. Kleinclauss, H. G. van der Poel, C. G. Stief, J. Rassweiler, G. Salomon, E. Solsona, A. Alcaraz, T. T. Tammela, D. J. Rosario, F. Gomez-Veiga, G. Ahlgren, F. Benzaghou, B. Gaillac, B. Amzal, F. M. J. Debruyne, G. Fromont, C. Gratzke, M. Emberton, "Padeliporfin vascular-targeted photodynamic therapy versus active surveillance in men with low-risk prostate cancer (CLIN1001 PCM301): an open-label, phase 3, randomised controlled trial," *Lancet Oncol.* **18**(2), 181–191 (2017).
14. A. Kawczyk-Krupka, A. M. Bugaj, M. Potempa, K. Wasilewska, W. Latos, A. Sieron, "Vascular-targeted photodynamic therapy in the treatment of neovascular age-related macular degeneration: clinical perspectives," *Photodiagnosis Photodyn. Ther.* **12**(2), 161–175 (2015).
15. A. Kawczyk-Krupka, K. Wawrzyniec, S. K. Musiol, M. Potempa, A. M. Bugaj, A. Sieron, "Treatment of localized prostate cancer using WST-09 and WST-11 mediated vascular targeted photodynamic therapy-A review," *Photodiag. Photodyn. Ther.* **12**(4), 567–574 (2015).
16. H. Qiu, Y. Zhou, Y. Gu, Q. Ang, S. Zhao, Y. Wang, J. Zeng, N. Huang, "Monitoring microcirculation changes in port wine stains during vascular targeted photodynamic therapy by laser speckle imaging," *Photochem. Photobiol.* **88**(4), 978–984 (2012).
17. A. T. Khalaf, Y. Sun, F. Wang, M. Sheng, Y. Li, X. Liu, "Photodynamic therapy using HMME for port-wine stains: clinical effectiveness and sonographic appearance," *Biomed Res. Int.* **2020**, 6030581 (2020).
18. Y. Huang, J. Yang, L. Sun, L. Zhang, M. Bi, "Efficacy of influential factors in hemoporfin-mediated photodynamic therapy for facial port-wine stains," *J. Dermatol.* **48**(11), 1700–1708 (2021).
19. Y. Lin, W. Gong, J. Kang, Y. Fang, J. Liu, L. Lin, X. Xiao, "Hemoporfin-mediated photodynamic therapy for port-wine stains: multivariate analysis of clinical efficacy and optical coherence tomography appearance," *Front. Med. (Lausanne)* **9**, 800836 (2022).
20. Y. Wang, Y. Gu, Z. Zuo, N. Huang, "Choosing optimal wavelength for photodynamic therapy of port wine stains by mathematic simulation," *J. Biomed. Opt.* **16**(9), 098001 (2011).
21. R. Shi, W. Feng, C. Zhang, Z. Zhang, D. Zhu, "FSOCA-induced switchable footpad skin optical clearing window for blood flow and cell imaging *in vivo*," *J. Biophoton.* **10**(12), 1647–1656 (2017).
22. V. Tuchin, D. Zhu, E. Genina, *Handbook of Tissue Optical Clearing: New Prospects in Optical Imaging*, 1st Edition, CRC Press, USA (2022).
23. B. K. B. Shariati, S. S. Khatami, M. A. Ansari, F. Jahangiri, H. Latifi, V. V. Tuchin, "Method for tissue clearing: temporal tissue optical clearing," *Biomed. Opt. Exp.* **13**(8), 4222–4235 (2022).
24. R. Shi, L. Guo, C. Zhang, W. Feng, P. Li, Z. Ding, D. Zhu, "A useful way to develop effective *in vivo* skin optical clearing agents," *J. Biophoton.* **10**(6–7), 887–895 (2017).
25. Y. Liu, D. Zhu, J. Xu, Y. Wang, W. Feng, D. Chen, Y. Li, H. Liu, X. Guo, H. Qiu, Y. Gu, "Penetration-enhanced optical coherence tomography angiography with optical clearing agent for clinical evaluation of human skin," *Photodiagnosis Photodyn. Ther.* **30**, 101734 (2020).
26. L. Pires, V. Demidov, B. C. Wilson, A. G. Salvio, L. Moriyama, V. S. Bagnato, I. A. Vitkin, C. Kurachi, "Dual-agent photodynamic therapy with optical clearing eradicates pigmented melanoma in preclinical tumor models," *Cancers (Basel)* **12**(7), 1956 (2020).
27. L. P. Martinelli, I. Iermak, L. T. Moriyama, M. B. Requena, L. Pires, C. Kurachi, "Optical clearing agent increases effectiveness of photodynamic therapy in a mouse model of cutaneous melanoma: an analysis by Raman microspectroscopy," *Biomed. Opt. Exp.* **11**(11), 6516–6527 (2020).
28. L. Pires, V. Demidov, I. A. Vitkin, V. Bagnato, C. Kurachi, B. C. Wilson, "Optical clearing of melanoma *in vivo*: characterization by diffuse reflectance spectroscopy and optical coherence tomography," *J. Biomed. Opt.* **21**(8), 081210 (2016).

29. G. M. Palmer, A. N. Fontanella, S. Shan, G. Hanna, G. Zhang, C. L. Fraser, M. W. Dewhirst, "*In vivo* optical molecular imaging and analysis in mice using dorsal window chamber models applied to hypoxia, vasculature and fluorescent reporters," *Nat. Protoc.* **6**(9), 1355–1366 (2011).
30. H. He, Y. Shen, B. Li, "Rapid skin optical clearing enhancement with salicylic acid for imaging blood vessels *in vivo*," *Photodiagnosis Photodyn. Ther.* **32**, 102005 (2020).
31. W. Feng, R. Shi, N. Ma, D. K. Tuchina, V. V. Tuchin, D. Zhu, "Skin optical clearing potential of disaccharides," *J. Biomed. Opt.* **21**(8), 081207 (2016).
32. P. C. Li, S. L. Ni, L. Zhang, S. Q. Zeng, Q. M. Luo, "Imaging cerebral blood flow through the intact rat skull with temporal laser speckle imaging," *Opt. Lett.* **31**(12), 1824–1826 (2006).
33. J. Xu, S. Song, Y. Li, R. K. Wang, "Complex-based OCT angiography algorithm recovers microvascular information better than amplitude- or phase-based algorithms in phase-stable systems," *Phys. Med. Biol.* **63**(1), 015023 (2017).
34. J. N. Mehrabi, J. Holmes, M. Abrouk, J. V. Wang, H. Pomerantz, A. M. Palma, C. B. Zachary, R. G. Geronemus, J. S. Waibel, K. M. Kelly, "Vascular characteristics of port wine birthmarks as measured by dynamic optical coherence tomography," *J. Am. Acad. Dermatol.* **85**(6), 1537–1543 (2021).
35. A. Latrive, L. R. Teixeira, A. S. Gomes, D. M. Zezell, "Characterization of skin port-wine stain and hemangioma vascular lesions using Doppler OCT," *Skin Res. Technol.* **22**(2), 223–229 (2016).
36. Z. Tan, J. Zhang, X. Niu, L. Lin, B. Li, "Monitoring Blood Flow During Vascular-Targeted Photodynamic Therapy Using Laser Speckle Imaging," *2016 Asia Commun. Photonics Conf. (ACP)*, 2–5 November, Wuhan, China, pp. 1–3 (2016).
37. J. Zhang, Z. Tan, X. Niu, L. Lin, H. Lin, B. Li, "Blood vessel damage correlated with irradiance for *in vivo* vascular targeted photodynamic therapy," *Proc. SPIE* **10024**, 100244N (2016).
38. J. Channual, B. Choi, K. Osann, D. Pattanachinda, J. Lotfi, K. M. Kelly, "Vascular effects of photodynamic and pulsed dye laser therapy protocols," *Lasers Surg. Med.* **40**(9), 644–650 (2008).
39. T. K. Smith, B. Choi, J. C. Ramirez-San-Juan, J. S. Nelson, K. Osann, K. M. Kelly, "Microvascular blood flow dynamics associated with photodynamic therapy, pulsed dye laser irradiation and combined regimens," *Lasers Surg. Med.* **38**(5), 532–539 (2006).
40. J. Wang, Y. Liang, S. Zhang, Y. Zhou, H. Ni, Y. Li, "Evaluation of optical clearing with the combined liquid paraffin and glycerol mixture," *Biomed. Opt. Exp.* **2**(8), 2329–2338 (2011).
41. V. Tuchin, I. Maksimova, D. Zimnyakov, I. Kon, A. Mavlyutov, A. Mishin, "Light propagation in tissues with controlled optical properties," *J. Biomed. Opt.* **2**(4), 401–417 (1997).
42. C. J. Chang, S. M. Cheng, J. S. Nelson, "Microvascular effects of Photofrin((R))-induced photodynamic therapy," *Photodiagnosis Photodyn. Ther.* **4**(2), 95–99 (2007).
43. B. Chen, B. W. Pogue, P. J. Hoopes, T. Hasan, "Vascular and cellular targeting for photodynamic therapy," *Crit. Rev. Eukaryot. Gene Expr.* **16**(4), 279–305 (2006).
44. I. Costantini, R. Cicchi, L. Silvestri, F. Vanzi, F. S. Pavone, "*In-vivo* and *ex-vivo* optical clearing methods for biological tissues: review," *Biomed. Opt. Exp.* **10**(10), 5251–5267 (2019).
45. T. Tian, Z. Yang, X. Li, "Tissue clearing technique: Recent progress and biomedical applications," *J. Anat.* **238**(2), 489–507 (2021).